Reduction of π-Bound Nitriles to π-Bound Imines in a Tungsten(II) Bis(acetylacetonate) Coordination Sphere

Andrew B. Jackson, Chetna Khosla, Helen E. Gaskins, Peter S. White, and Joseph L. Templeton*

W.R. Kenan Laboratory, Department of Chemistry, University of North Carolina, Chapel Hill, North Carolina 27599-3290

Received September 10, 2007

Addition of MeOTf (OTf = CF_3SO_3) to complexes of the type W(CO)(acac)$_2$(η^2-N≡CR) (acac = acetylacetonate) [R = Ph (**1a**), Me (**1b**)] yields cationic iminoacyl triflate salts of the type [W(CO)(acac)$_2$(η^2-MeN═CR)][OTf]. Complexes **2a** and **2b** undergo nucleophilic attack at the iminoacyl carbon with Na[HB(OMe)$_3$] or MeMgBr to form neutral η^2-imine complexes of the type W(CO)(acac)$_2$[η^2-MeN═C(Nuc)R] [Nuc = H (**3a, 3b**), Me (**4**)]. Hydride addition to **2b** results in W(CO)(acac)$_2$(η^2-MeN═CHMe), **3b**, a complex that exhibits interconversion of diastereomers at ambient temperature on the NMR time scale. X-ray structures of cationic iminoacyl complex **2a** and neutral imine complex **4** confirm η^2-C═N bonding of both the iminoacyl and imine ligands.

Introduction

The majority of organometallic nitrile complexes demonstrate σ-bonding of the nitrile, in which the nitrile carbon is susceptible to nucleophilic attack.[1,2] Metal-mediated hydrolysis of nitriles to amides and on to carboxylic acids involves initial hydroxide attack at the nitrile carbon.[1–6] Reduction from a nitrile to an amine can be accomplished via alternating nucleophilic attack at carbon and protonation at nitrogen beginning with initial hydride attack at the nitrile carbon.[7]

Less is known about the chemistry of π-bound nitriles. Although rare compared to their σ-bound counterparts, π-bound nitrile complexes have been known for two decades.[8–23] We recently reported the reaction of W(CO)$_3$(acac)$_2$[24] with nitriles to form complexes of the type W(CO)(acac)$_2$(η^2-N≡CR), where the nitrile acts as a four-electron donor ligand to tungsten.[25]

Coordination of the RC≡N triple bond leaves the nitrile susceptible to alkylation at the nucleophilic nitrogen lone pair, resulting in cationic η^2-iminoacyl complexes.[21–23] A number of neutral π-bound iminoacyl complexes are known,[26–39] but cationic complexes that offer enhanced reactivity toward nu-

* To whom correspondence should be addressed. E-mail: joetemp@unc.edu.

(1) Kukushkin, V. Y.; Pombeiro, A. J. L. *Chem. Rev.* **2002**, *102*, 1771.
(2) Michelin, R. A.; Mozzon, M.; Bertani, R. *Coord. Chem. Rev.* **1996**, *147*, 299.
(3) Parkins, A. W. *Platinum Met. Rev.* **1996**, *40*, 169.
(4) daRocha, Z. N.; Chiericato, G.; Tfouni, E. *Electron Transfer Reactions* American Chemical Society:Washington, D.C., 1997; Vol. 253.
(5) Murahashi, S. I.; Takaya, H. *Acc. Chem. Res.* **2000**, *33*, 225.
(6) Kukushkin, V. Y.; Pombeiro, A. J. L. *Inorg. Chim. Acta* **2005**, *358*, 1.
(7) Feng, S. G.; Templeton, J. L. *J. Am. Chem. Soc.* **1989**, *111*, 6477.
(8) Wright, T. C.; Wilkinson, G.; Motevalli, M.; Hursthouse, M. B. *J. Chem. Soc., Dalton Trans.* **1986**, 2017.
(9) Chetcuti, P. A.; Knobler, C. B.; Hawthorne, M. F. *Organometallics* **1988**, *7*, 650.
(10) Barrera, J.; Sabat, M.; Harman, W. D. *J. Am. Chem. Soc.* **1991**, *113*, 8178.
(11) Barrera, J.; Sabat, M.; Harman, W. D. *Organometallics* **1993**, *12*, 4381.
(12) Lorente, P.; Carfagna, C.; Etienne, M.; Donnadieu, B. *Organometallics* **1996**, *15*, 1090.
(13) Kiplinger, J. L.; Arif, A. M.; Richmond, T. G. *Chem. Commun.* **1996**, 1691.
(14) Thomas, S.; Tiekink, E. R. T.; Young, C. G. *Organometallics* **1996**, *15*, 2428.
(15) Kiplinger, J. L.; Arif, A. M.; Richmond, T. G. *Organometallics* **1997**, *16*, 246.
(16) Thomas, S.; Young, C. G.; Tiekink, E. R. T. *Organometallics* **1998**, *17*, 182.
(17) Garcia, J. J.; Jones, W. D. *Organometallics* **2000**, *19*, 5544.
(18) Garcia, J. J.; Brunkan, N. M.; Jones, W. D. *J. Am. Chem. Soc.* **2002**, *124*, 9547.
(19) Garcia, J. J.; Arévalo, A.; Brunkan, N. M.; Jones, W. D. *Organometallics* **2004**, *23*, 3997.
(20) Etienne, M.; Carfagna, C.; Lorente, P.; Mathieu, R.; de Montauzon, D. *Organometallics* **1999**, *18*, 3075.
(21) Shin, J. H.; Savage, W.; Murphy, V. J.; Bonanno, J. B.; Churchill, D. G.; Parkin, G. *J. Chem. Soc., Dalton Trans.* **2001**, 1732.
(22) Cross, J. L.; Garrett, A. D.; Crane, T. W.; White, P. S.; Templeton, J. L. *Polyhedron* **2004**, *23*, 2831.
(23) Lis, E. C.; Delafuente, D. A.; Lin, Y. Q.; Mocella, C. J.; Todd, M. A.; Liu, W. J.; Sabat, M.; Myers, W. H.; Harman, W. D. *Organometallics* **2006**, *25*, 5051.
(24) Jackson, A. B.; White, P. S.; Templeton, J. L. *Inorg. Chem.* **2006**, *45*, 6205.
(25) Jackson, A. B.; Schauer, C. K.; White, P. S.; Templeton, J. L. *J. Am. Chem. Soc.* **2007**, *129*, 10628.
(26) Adams, R. D.; Chodosh, D. F. *J. Am. Chem. Soc.* **1977**, *99*, 6544.
(27) Adams, R. D.; Chodosh, D. F. *Inorg. Chem.* **1978**, *17*, 41.
(28) Gamble, A. S.; Birdwhistell, K. R.; Templeton, J. L. *J. Am. Chem. Soc.* **1990**, *112*, 1818.
(29) McMullen, A. K.; Rothwell, I. P.; Huffman, J. C. *J. Am. Chem. Soc.* **1985**, *107*, 1072.
(30) Chamberlain, L. R.; Durfee, L. D.; Fanwick, P. E.; Kobriger, L.; Latesky, S. L.; McMullen, A. K.; Rothwell, I. P.; Folting, K.; Huffman, J. C.; Streib, W. E.; Wang, R. *J. Am. Chem. Soc.* **1987**, *109*, 390.
(31) Lubben, T. V.; Plössl, K.; Norton, J. R.; Miller, M. M.; Anderson, O. P. *Organometallics* **1992**, *11*, 122.
(32) Zambrano, C. H.; Fanwick, P. E.; Rothwell, I. P. *Organometallics* **1994**, *13*, 1174.
(33) Daff, P. J.; Monge, A.; Palma, P.; Poveda, M. L.; Ruiz, C.; Valerga, P.; Carmona, E. *Organometallics* **1997**, *16*, 2263.
(34) Scott, M. J.; Lippard, S. J. *Organometallics* **1997**, *16*, 5857.
(35) Sánchez-Nieves, J.; Royo, P.; Pellinghelli, M. A.; Tiripicchio, A. *Organometallics* **2000**, *19*, 3161.
(36) Sánchez-Nieves, J.; Royo, P.; Mosquera, M. E. G. *Eur. J. Inorg. Chem.* **2006**, 127.
(37) Suzuki, E.; Komuro, T.; Okazaki, M.; Tobita, H. *Organometallics* **2007**, *26*, 4379.
(38) Guram, A. S.; Jordan, R. F. *J. Org. Chem.* **1993**, *58*, 5595.
(39) Durfee, L. D.; Rothwell, I. P. *Chem. Rev.* **1988**, *88*, 1059.
(40) Yoshida, T.; Hirotsu, K.; Higuchi, T.; Otsuka, S. *Chem. Lett.* **1982**, 1017.

10.1021/om7009039 CCC: $40.75
Publication on Web 02/22/2008

Scheme 1. Addition of Alkyl Triflate to η^2-Nitrile Complexes

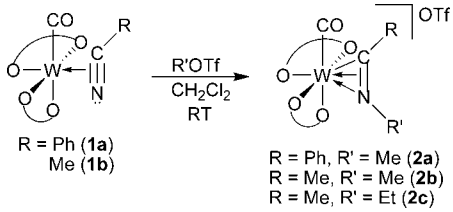

cleophiles are rare.[20–23,38–44] Common methods of formation of π-bound iminoacyl complexes include (1) migratory insertion of isocyanide into a metal−alkyl or a metal−hydride bond[39] and (2) addition of alkyl halides to anionic isocyanide complexes.[26–28] Reactivity studies with the cationic π-bound iminoacyl complexes have shown them to be agile reagents susceptible to nucleophilic attack at the iminoacyl carbon to form η^2-imines.[34,39,45–47]

We now report addition of strong alkylating reagents R′OTf (R′ = Me, Et) to π-bound nitrile ligands to form cationic iminoacyl-carbonyl complexes, [W(CO)(acac)$_2$(η^2-R′N═CR)][OTf]. Nucleophilic addition at the iminoacyl carbon of the cationic complex forms η^2-imines of the type W(CO)(acac)$_2$(η^2-R′N═CRR″) (R″ = H, Me). This is the first example of stepwise addition of an electrophile and a nucleophile to an η^2-nitrile.

Results and Discussion

Combining stoichiometric amounts of W(CO)(acac)$_2$(η^2-N≡CPh) (**1a**) and MeOTf in methylene chloride at room temperature generates [W(CO)(acac)$_2$(η^2-MeN═CPh)][OTf] (**2a**) (Scheme 1). In situ IR spectroscopy indicates the presence of a single carbon monoxide absorbance at 1985 cm^{-1} in the product, an increase of approximately 90 cm^{-1} from the starting material. Alkylation of alkyl or aryl nitriles gives similar results. Addition of either MeOTf or EtOTf to W(CO)(acac)$_2$(η^2-N≡CMe) (**1b**) generates W(CO)(acac)$_2$(η^2-R′N═CMe)][OTf] [R′═Me (**2b**), Et (**2c**)].

The ^{1}H NMR spectrum of complex **2a** shows a downfield resonance at 4.97 ppm attributed to the newly added methyl group on nitrogen. Complex **2b** displays similar NMR results: the methyl bound to nitrogen resonates at 4.79 ppm, while the methyl group bound to carbon resonates at 4.11 ppm, shifted downfield from 3.71 in the neutral η^2-acetonitrile precursor **1b**. Each methyl peak associated with the iminoacyl ligand in **2b** appears as a sharp singlet at room temperature. As confirmed by an HMQC experiment, the iminoacyl carbon in **2b** appears at 233.1 ppm in the ^{13}C NMR spectrum, downfield from 208.7 ppm in the neutral η^2-acetonitrile adduct. The carbonyl carbon shifts upfield to 219.7 ppm from 237.6 ppm in the precursor acetonitrile complex.[25]

The solid state structure of cationic η^2-iminoacyl complex **2a** (Figure 1) shows two acetylacetonate chelates and one carbon monoxide ligand bound to tungsten defining five coordination sites of an approximate octahedron. The sixth site is filled with an iminoacyl ligand located cis to carbon monoxide with the nitrogen atom positioned distal to the carbonyl ligand. The N═C bond of the η^2-iminoacyl ligand is parallel to the W−C≡O axis, reminiscent of the C≡N orientation observed in the nitrile complex.[25] The tungsten−nitrogen bond distance, W1−N4, decreases slightly from 2.018(5) Å in the nitrile complex to 1.977(7) Å, and the bond distance to the iminoacyl carbon, W1−C5, increases slightly from 2.038(5) to 2.069(8) Å. The carbon−nitrogen bond distance (1.283(10) Å) remains virtually unchanged from the value observed for the analogous bond in the nitrile complex (1.270(7) Å).[25] In summary, formal addition of a cationic methyl group to the lone pair of the η^2-nitrile nitrogen does little to distort the geometry of the robust W−C−N triangle.

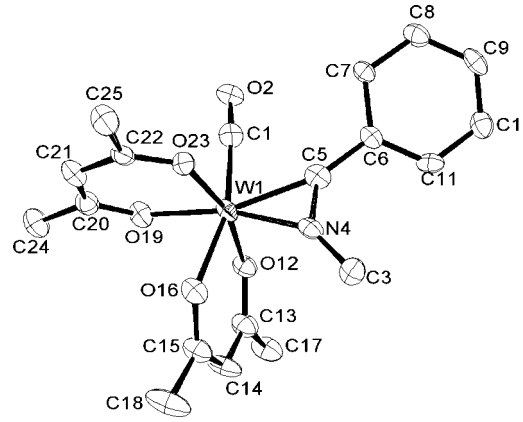

Figure 1. ORTEP diagram of [W(CO)(acac)$_2$(η^2-MeN═CPh)][OTf] (**2a**). Thermal ellipsoids are drawn with 50% probability. Hydrogen atoms and triflate counterion omitted for clarity.

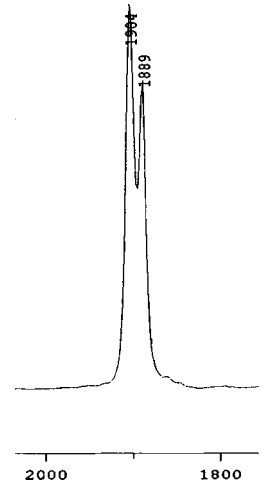

Figure 2. Expanded IR spectrum of W(CO)(acac)$_2$(η^2-MeN═CHPh) (**3a**) in hexanes showing the CO absorption frequency of both diastereomers.

Addition of Na[HB(OMe)$_3$] to [W(CO)(acac)$_2$(MeN═CPh)][OTf] (**2a**) in THF at −78 °C reduces the iminoacyl ligand to a coordinated imine in W(CO)(acac)$_2$(η^2-MeN═CHPh) (**3a**) via nucleophilic attack of hydride at the iminoacyl carbon (Scheme 2). The room temperature ^{1}H NMR spectrum shows two diastereomers in a 2:1 ratio, reflecting chirality at both tungsten and carbon. The *N*-methyl on the imine ligand shifts upfield to 3.71 ppm (major) from 4.97 ppm in the cationic complex. Two resonances attributed to the imine C−*H* appear

(41) Carrier, A. M.; Davidson, J. G.; Barefield, E. K.; Van Derveer, D. G. *Organometallics* **1987**, *6*, 454.
(42) Añtinolo, A.; Fajardo, M.; Gil-Sanz, R.; López-Mardomingo, C.; Martín-Villa, P.; Otero, A.; Kubicki, M. M.; Mugnier, Y.; El Krami, S.; Mourad, Y. *Organometallics* **1993**, *12*, 381.
(43) Temme, B.; Erker, G. *J. Organomet. Chem.* **1995**, *488*, 177.
(44) Cook, K. S.; Piers, W. E.; Patrick, B. O.; McDonald, R. *Can. J. Chem.* **2003**, *81*, 1137.
(45) Galakhov, M. V.; Gómez, M.; Jiménez, G.; Royo, P.; Pellinghelli, M. A.; Tiripicchio, A. *Organometallics* **1995**, *14*, 1901.
(46) Durfee, L. D.; Fanwick, P. E.; Rothwell, I. P.; Folting, K.; Huffman, J. C. *J. Am. Chem. Soc.* **1987**, *109*, 4720.
(47) Chiu, K. W.; Jones, R. A.; Wilkinson, G.; Galas, A. M. R.; Hursthouse, M. B. *J. Chem. Soc., Dalton Trans.* **1981**, 2088.

Scheme 2. Addition of Sodium Trimethoxyborohydride to Cationic Iminoacyl Complexes

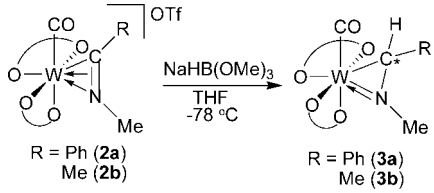

between 5 and 6 ppm, the same region as the acac methines. A COSY experiment shows the imine C−*H* peaks at 5.56 (major) and 5.80 (minor) ppm. The ^{13}C NMR spectrum displays the imine carbon at 60.8 (major) and 57.2 (minor) ppm, an upfield shift of ∼170 ppm from the iminoacyl carbon in complex **2a**. This significant change in the ^{13}C chemical shift reflects the sp^3 character of the imine carbon in complex **3a**. IR spectroscopy of **3a** in hexanes also indicates two isomers with carbonyl C≡O absorptions at 1904 and 1889 cm^{-1} (Figure 2). Addition of a nucleophilic methyl group to **2a** with MeMgBr as a reagent produces W(CO)(acac)$_2$(η^2-MeN═CMePh) (**4**) (Scheme 3).

The X-ray structure of **4** (Figure 3) depicts the same framework around the metal as is observed in the neutral nitrile and cationic iminoacyl carbonyl complexes: two acetylacetonate chelates and one carbon monoxide ligand surround tungsten with an η^2-N═C linkage in the remaining position. The chiral imine

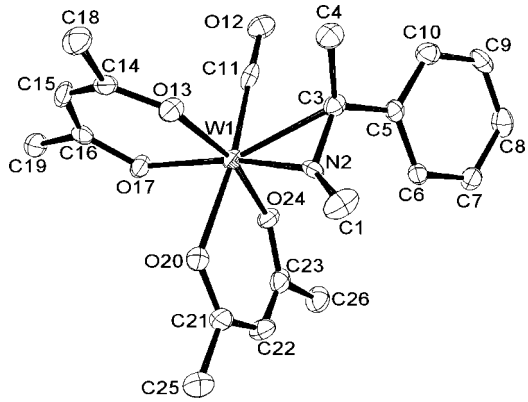

Figure 3. ORTEP diagram of W(CO)(acac)$_2$(η^2-MeN═CMePh) (**4**). Thermal ellipsoids are drawn with 50% probability. Hydrogen atoms are omitted for clarity.

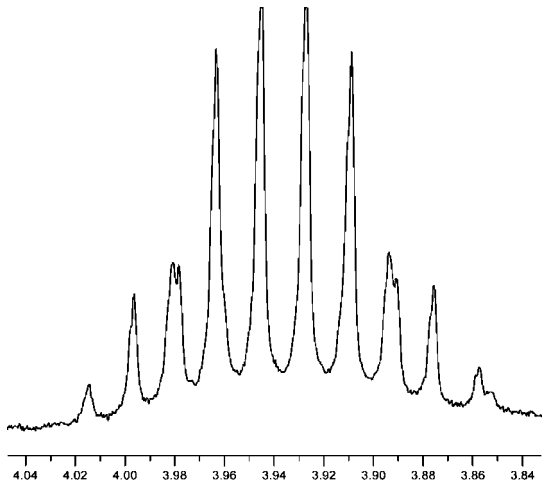

Figure 4. Expanded room temperature ^{1}H NMR (CD_2Cl_2) spectrum of W(CO)(acac)$_2$(η^2-EtN═CMeMe), **5**, showing the ABX$_3$ splitting pattern attributed to the diastereotopic methylene protons on the imine ligand.

Scheme 3. Addition of Methylmagnesium Bromide to 2a

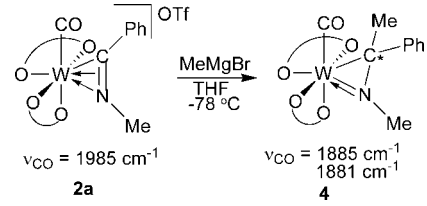

ligand is π-bound to the metal center, cis to carbon monoxide, with the nitrogen atom distal to the metal–carbonyl ligand. Both substituents on the imine carbon skew from the plane defined by the W−C−N triangle in accord with an aziridine geometry. The methyl group bound to nitrogen deviates only slightly from the same plane. Bond distances from the metal to the imine ligand reflect a large change in the geometry of the W−C−N triangle upon addition of a nucleophile at carbon. The tungsten−carbon bond, W1−C3, lengthens considerably from 2.069(8) to 2.274(2) Å, and the W1−N2 bond decreases from 1.977(7) to 1.905(5) Å, suggestive of lone pair donation from the nitrogen to tungsten, effectively resulting in a double bond from nitrogen to the metal. The carbon−nitrogen bond distance in the imine ligand, N2−C3, elongates from 1.283(10) to 1.383(2) Å, indicating a loss of C−N multiple bond character upon nucleophilic attack. These values mirror those of W(CO)(acac)$_2$(η^2-PhN═CHPh), an imine complex derived from direct addition of an *N*-benzylideneaniline to W(CO)$_3$(acac)$_2$.[25] *Note that no rearrangement in W−C−N connectivity occurs in the transformation from nitrile to iminoacyl and on to imine.* Each η^2-C═N ligand remains π-bound to tungsten in the same orientation of the ligating carbon and nitrogen atoms relative to the rest of the unaltered coordination sphere.

Addition of Na[HB(OMe)$_3$] to **2b** appears to proceed like the other addition reactions, but room temperature ^{1}H NMR spectroscopy does not indicate the presence of two diastereomers in solution. In fact, signals due to the added hydrogen and the methyl of the anticipated H−C−Me unit of the imine are absent at room temperature. However, low-temperature ^{1}H NMR spectroscopy reveals that hydride addition indeed occurs to produce W(CO)(acac)$_2$(η^2-MeN═CHMe) (**3b**). At 238 K, two diastereomers are resolved and appear in a 1:1 ratio. The added hydrogen atom is bound to the imine carbon and appears as a quartet at either 4.55 or 5.11 ppm due to the presence of two diastereomers. Variable-temperature NMR measurements focusing on the two singlets for the methyl group bound to nitrogen in the two diastereomers reveal a coalescence temperature of 263 K. By using the Gutowsky−Holm equation,[48] this temperature corresponds to a free energy barrier for diastereomer interconversion of $\Delta G^{\ddagger} = 13.2$ kcal/mol. The fluxional process observed at room temperature results from interconversion of the two diastereomers on the NMR time scale. This dynamic behavior is observed in the CHMe (**3b**) derivative, but not in the CHPh (**3a**) or the CMePh (**4**) derivatives.

For this interconversion process to occur, one of the two stereocenters in the molecule must racemize. One possible mechanism involves interconversion of chirality at the imine carbon (Scheme 4, Pathway A). Dissociation of the carbon atom from the tungsten center could form a 16-electron intermediate species in which the imine is σ-bound through the nitrogen atom. Once the imine assumes the planar geometry appropriate for an N-bound ligand, the carbon can coordinate to tungsten

(48) Gutowsky, H. S.; Holm, C. H. *J. Chem. Phys.* **1956**, *25*, 1228.

Scheme 4. Possible Mechanisms for Interconversion of Diastereomers in 3b

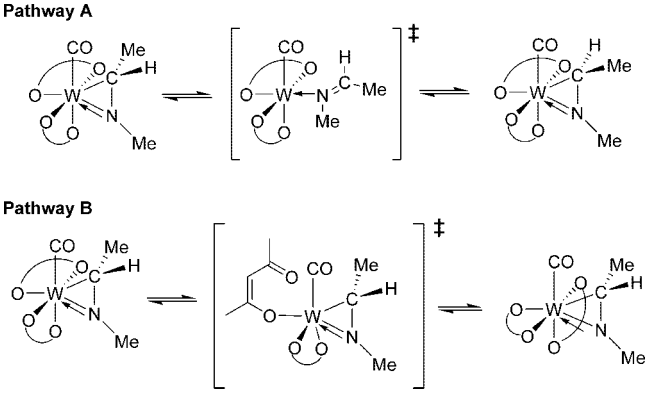

Scheme 5. Synthetic Route To Generate Nonchiral Imine Derivative 5

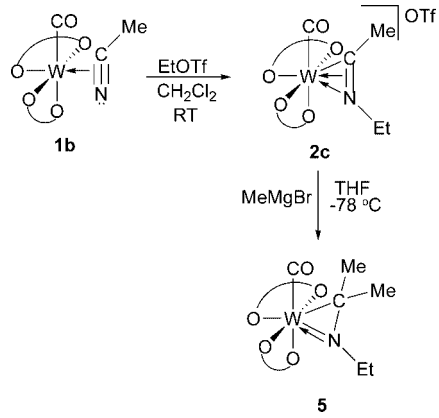

Table 1. Comparison of Salient Bond Distances, NMR, and IR Data

complex	W−N (Å)	W−C (Å)	C−N (Å)	^{13}C, N≡*C* (δ)	IR, ν_{CO} (cm^{-1})
nitrile[25]	2.018(5)	2.038(5)	1.270(7)	211.2	1895
iminoacyl (**2a**)	1.977(7)	2.069(8)	1.283(10)	226.2	1976
imine (**4**)	1.905(5)	2.274(2)	1.383(2)	59.3, 60.6	1881, 1885

through either face. Note that the geometry of the η^2-coordinated imine requires rotation of the CHMe fragment relative to the C═N−Me plane of the κ^1-N-imine upon binding the imine carbon to tungsten.

A second possibility for isomer interconversion involves inversion of stereochemistry at tungsten via dissociation of an acetylacetonate arm resulting in a 16-electron intermediate species (Scheme 4, Pathway B). Reassociation of the chelate arm on the opposite side of the metal atom inverts stereochemistry at the tungsten center.

To distinguish between these two possible mechanisms, an imine derivative deprived of a chiral center at the imine carbon was synthesized, and an ethyl substituent on the imine nitrogen was used to probe chirality at the metal using the diastereotopic methylene protons. W(CO)(acac)$_2$[η^2-EtN═CMe$_2$], **5**, was synthesized by alkylation of **1b** with EtOTf, follwed by subsequent nucleophilic attack on the cationic complex with MeMgBr (Scheme 5). At room temperature, the ^{1}H NMR spectrum shows one product, with a distinct ABX$_3$ pattern corresponding to the methylene protons on the nitrogen-ethyl substituent (Figure 4). Detection of a chiral environment by the diastereotopic methylene protons at room temperature eliminates facile acetylacetonate dechelation as a mechanism for accessing an intermediate with a mirror plane in this complex and makes it unlikely that acac rearrangement is the dynamic process responsible for diastereomer interconversion in complex **3b**. Dissociation of the imine ligand at carbon to form a κ^1-N-imine with a chiral tungsten center becomes the likely mechanism for the dynamic process that interconverts diastereomers in **3b**.

In summary, stepwise conversion of π-bound nitriles to π-bound imines has been accomplished. Single-crystal X-ray structures have been determined for the cationic iminoacyl complex [W(CO)(acac)$_2$(η^2-MeN═CPh)][OTf], **2a**, and the neutral imine complex W(CO)(acac)$_2$(η^2-MeN═CMePh), **4**. Complex **3b,**W(CO)(acac)$_2$(η^2-MeN═CHMe), displays fluxionality, which interconverts diastereomers via dissociation of the η^2-imine carbon.

Table 2. Crystal Data and Refinement Parameters for 2a and 4

complex	**2a**	**4**
empirical formula	$C_{20}H_{22}F_3NO_8SW$	$C_{20}H_{25}NO_5W$
fw	677.29	543.26
color	burgundy	dark red
tem p(K)	100(2)	100(2)
λ(Mo Kα) (Å)	0.71703	0.71703
cryst syst	monoclinic	monoclinic
space group	*C*2/*c*	$P2_1/n$
a (Å)	28.4062(13)	8.3192(3)
b (Å)	7.6114(3)	14.2955(4)
c (Å)	22.3725(10)	17.0591(6)
α (deg)	90	90
β (deg)	98.730(3)	92.92
γ (deg)	90	90
Vol. (Å^3)	4781.1(4)	2026.15(12)
Z	8	4
D_{calc} (Mg/m^3)	1.882	1.781
μ (mm^{-1})	4.99	5.73
F(000)	2638	1064
cryst size (mm)	0.20 × 0.05 × 0.01	0.10 × 0.10 × 0.10
2*θ* range (deg)	5.00 to 50.00	1.86 to 30.07
no. of reflns collected	30525	88084
no. of independent reflns	4229 [*R*(int) = 0.0550]	88084 [*R*(int) = 0.0000]
data/restraints/parameters	4229/0/308	88084/0/252
goodness-of-fit on F^2	1.9382	1.004
final *R* indices [$I > 2\sigma(I)$]	$R_1 = 0.040$ $wR_2 = 0.042$	$R_1 = 0.0394$ $wR_2 = 0.1014$
R indices (all data)	$R_1 = 0.056$ $wR_2 = 0.044$	$R_1 = 0.0530$ $wR_2 = 0.1065$

Experimental Section

General Information. Reactions were performed under a dry nitrogen atmosphere with standard Schlenk techniques. Methylene chloride, hexanes, and pentane were purified by passage through an activated alumina column under a dry argon atmosphere.[49] THF was distilled from a sodium ketal suspension. Methylene chloride-d_2 was dried over CaH_2 and degassed. All other reagents were purchased from commercial sources and were used without further purification.

NMR spectra were recorded on Bruker DRX400, AMX400, or AMX300 spectrometers. Infrared spectra were recorded on an ASI Applied Systems React IR 1000 FT-IR spectrometer. Elemental analysis was performed by Atlantic Mircrolab, Norcross, GA, and Robertson Microlit, Madison, NJ. **1a** and **1b** were made in accordance with a literature procedure.[25]

[W(CO)(acac)$_2$(η^2-MeN═CPh)][OTf] (2a). A 200-mL Schlenk flask was charged with **1a** (1.08 g) and the solid was dissolved in

(49) Pangborn, A. B.; Giardello, M. A.; Grubbs, R. H.; Rosen, R. K.; Timmers, F. J. *Organometallics* **1996**, *15*, 1518.

methylene chloride (30 mL) resulting in a dark amber solution. Treatment with 1.5 equiv of methyl trifluoromethylsulfonate (MeOTf) caused a color change to burgundy. In situ IR spectroscopy revealed a single CO absorbance at ~1985 cm^{-1}after 30 min of stirring. The solvent volume was reduced in vacuo and hexanes (50 mL) were added to precipitate the cationic product. Excess solvent was removed via cannula filtration yielding a burgundy powder (1.32 g, 93%). A portion of the isolated burgundy powder **2a** was dissolved in methylene chloride and layered with hexanes in an inert atmosphere at −30 °C. Small burgundy needles of **2a** suitable for X-ray analysis formed overnight. IR (KBr): ν_{CO} = 1976 cm^{-1}, ν_{CN} = 1627 cm^{-1}. ^{1}H NMR (CD_2Cl_2, 298 K, δ): 7.88–7.90 (m, 2H, *o*-C_6H_5), 7.80–7.84 (m, 2H, *m*-C_6H_5), 7.69–7.73 (m, 1H, *p*-C_6H_5), 5.95, 5.94 (each a s, each 1H, acac C–*H*), 4.97 (s, 3H, N−CH_3), 2.58, 2.38, 2.37, 2.16 (each a s, each 3H, acac CH_3). ^{13}C{^{1}H} NMR (CD_2Cl_2, 298 K, δ): 25.4, 26.3, 26.6, 28.4 (acac *C*H_3), 42.3 (N-*C*H_3), 101.6, 104.3 (acac *C*H), 128.0 (*ipso*-C_6H_5), 130.1 (*m*-C_6H_5), 132.1 (*o*-C_6H_5), 136.7 (*p*-C_6H_5), 187.8, 188.9, 193.3, 199.0 (acac *C*O), 220.8 (*C*≡O), 226.2 (N≡*C*). Anal. Calcd for $WC_{20}H_{22}O_8NSF_3$: C, 35.46; H, 3.28; N, 2.07. Found: C, 35.14; H, 3.14; N, 1.99.

[W(CO)(acac)$_2$(η^2-MeN=CMe)][OTf] (2b). A 200-mL Schlenk flask was charged with **1b** (0.74 g) and the solid was dissolved in CH_2Cl_2 (20 mL) resulting in a dark amber solution. Treatment with 1 equiv of MeOTf caused a color change to olive green. In situ IR spectroscopy revealed a single CO absorbance at ~1985 cm^{-1}after 30 min of stirring. The solvent volume was reduced in vacuo and hexanes (50 mL) were added to precipitate the cationic product. Excess solvent was removed via cannula filtration yielding an olive green powder (740 mg, 75%). IR (KBr): ν_{CO} = 1968 cm^{-1}, ν_{CN} = 1657 cm^{-1}. ^{1}H NMR (CD_2Cl_2, 298 K, δ): 5.88, 5.87 (each a s, each 1H, acac C*H*), 4.79 (s, 3H, N−CH_3), 4.11 (s, 3H, N=C−CH_3), 2.53, 2.13 (each a s, each 3H, acac CH_3), 2.32 (s, 6H, acac CH_3); ^{13}C{^{1}H} NMR (CD_2Cl_2, 298 K, δ): 20.3 (N≡C−*C*H_3), 25.2, 26.1, 26.4, 28.1 (acac *C*H_3), 41.3 (N−*C*H_3), 101.7, 104.0 (acac *C*H), 187.5, 188.8, 193.3, 198.8 (acac *C*O), 219.7 (*C*≡O), 233.1 (N≡*C*). Anal. Calcd for $WC_{15}H_{20}O_8NSF_3$: C, 29.28; H, 3.28; N, 2.28. Found: C, 29.06; H, 3.01; N, 1.96.

[W(CO)(acac)$_2$(η^2-EtN=CMe)][OTf] (2c). A Schlenk flask was charged with **1b** (50 mg) and CH_2Cl_2 (20 mL). Ethyl triflate (30 μL) was added at 0 °C and the solution was stirred overnight at room temperature. The green solution was reduced and washed with hexanes to afford a green-brown powder (55 mg, 79%). ^{1}H NMR (CD_2Cl_2, 298 K, δ): 5.92, 5.87 (each a s, each 1H, acac C*H*), 5.17 (m, 2H, N−CH_2−CH$_3$), 4.13 (s, 3H, N≡C−CH_3), 2.52, 2.32, 2.30, 2.14 (each a s, each 3H, acac CH_3), 1.46 (t, 3H, N−CH$_2$−CH_3). ^{13}C{^{1}H} NMR (CD_2Cl_2, 298 K, δ): 15.0 (N−CH$_2$−*C*H$_3$), 20.6 (N≡C−*C*H_3), 25.4, 26.2, 26.4, 28.2 (acac *C*H_3), 51.8 (N−*C*H$_2$−CH$_3$), 101.6, 104.1 (acac *C*H), 187.7, 188.9, 193.2, 198.9 (acac *C*O), 219.5 (*C*≡O), 232.0 (N≡*C*).

W(CO)(acac)$_2$(η^2-MeN=CHPh) (3a). Under an inert atmosphere, **2a** (200 mg) was combined with sodium trimethoxyborohydride, Na[HB(OMe)$_3$] (40 mg), in a 200-mL Schlenk flask. The flask was cooled to −78 °C and THF (20 mL) was added. A color change from burgundy to cherry red occurred and in situ IR spectroscopy revealed a new CO absorbance at 1883 cm^{-1} after 10 min of stirring. The solvent was removed in vacuo and the resulting red solid was chromatographed on silica with CH_2Cl_2 to elute a red band (75 mg, 48%). IR (hexanes): ν_{CO} = 1904 cm^{-1} (major diastereomer), ν_{CO} = 1889 cm^{-1} (minor diastereomer). ^{1}H NMR (CD_2Cl_2, 298 K, δ, major diastereomer): 7.24–7.32 (m, 3H, *m* and *p*-C_6H_5), 7.14–7.16 (m, 2H, *o*-C_6H_5), 5.48, 5.72 (each a s, each 1H, acac C*H*), 5.56 (s, 1H, N−C−*H*), 3.71 (s, 3H, N−CH_3), 2.57, 2.25, 2.16, 2.03 (each a s, each 3H, acac CH_3). ^{1}H NMR (CD_2Cl_2, 298 K, δ, minor diastereomer): 7.01–7.07 (m, 3H, *m* and *p*-C_6H_5), 6.80–6.83 (m, 2H, *o*-C_6H_5), 5.80 (s, 1H, N−C−*H*), 5.58, 5.56 (each a s, each 1H, acac C*H*), 3.83 (s, 3H, N−CH_3), 2.49, 2.13, 2.09, 2.03 (each a s, each 3H, acac CH_3). ^{13}C{^{1}H} NMR (CD_2Cl_2, 298 K, δ, major diastereomer): 26.0, 26.3, 27.7, 27.9 (acac *C*H_3), 43.6 (N−*C*H_3), 60.8 (N−*C*), 99.4, 101.0 (acac *C*H), 127.4 (*m*-C_6H_5), 127.6 (*p*-C_6H_5), 127.9 (*o*-C_6H_5), 148.1 (*ipso*-C_6H_5), 184.3, 186.3, 187.0, 193.8 (acac *C*O), 233.4 (*C*≡O). ^{13}C{^{1}H} NMR (CD_2Cl_2, 298 K, δ, minor diastereomer): 25.7, 26.9, 27.5, 28.1 (acac *C*H_3), 43.8 (N−*C*H_3), 57.2 (N−*C*), 99.4, 101.5 (acac *C*H), 126.6 (*m*-C_6H_5), 126.7 (*o*-C_6H_5), 127.0 (*p*-C_6H_5), 147.2 (*ipso*-C_6H_5), 185.5, 185.6, 188.1, 194.7 (acac *C*O), 235.3 (*C*≡O). Anal. Calcd for $WC_{19}H_{23}O_5N$: C, 43.11; H, 4.39; N, 2.65. Found: C, 43.10; H, 4.34; N, 2.66.

W(CO)(acac)$_2$(η^2-MeN=CHMe) (3b). Under an inert atmosphere, **2b** (30 mg) was placed in a 100-mL Schlenk flask. The flask was cooled to −78 °C and THF (15 mL) was added. In a separate flask a solution containing Na[HB(OMe)$_3$] (7 mg) and THF (5 mL) was prepared and cannula transferred to the flask containing **2b** resulting in a color change from green to red. After 30 min of stirring, the solvent volume was reduced in vacuo and hexanes (20 mL) were added to precipitate residual salts. The red supernatant was cannula filtered to a separate flask and the remaining solvent was removed in vacuo yielding a red-brown solid (17 mg, 75%). ^{1}H NMR (CD_2Cl_2, 240 K, δ, 1:1 diastereomers): 5.64, 5.46, 5.43 (each a s, 2:1:1, acac C*H*), 5.11, 4.55 (each a q, 1H, N−C−*H*, $^2J_{H-H}$ = 4.9 Hz), 3.64, 3.57 (each a s, 3H, N−CH_3), 2.46, 2.45, 2.20, 2.06, 2.05, 2.00, 1.98 (each a s, 3:3:6:3:3:3:3, acac CH_3), 2.23, 1.96 (each a d, each 3H, N=C−CH_3, $^2J_{H-H}$ = 4.9 Hz). ^{13}C{^{1}H} NMR (CD_2Cl_2, 240 K, δ, 1:1 diastereomers): 19.4–28.1 (acac *C*H$_3$, N=C−*C*H$_3$), 41.2, 43.2 (N−*C*H_3), 56.4, 56.7 (N=*C*), 99.4, 99.5, 100.8, 100.9 (acac *C*H), 183.7, 184.1, 184.8, 185.4, 186.0, 186.1, 193.7, 194.1 (acac *C*O), 231.3, 231.9 (*C*≡O).

W(CO)(acac)$_2$(η^2-MeN=CMePh) (4). Under an inert atmosphere, **2a** (50 mg) was placed in a 100-mL Schlenk flask. The flask was cooled to −78 °C and THF (10 mL) was added. A solution of methyl magnesiumbromide, MeMgBr (30 μL, 3 M in Et_2O), was added to the flask. After 10 min of stirring, in situ IR spectroscopy indicated the presence of one CO absorbance at 1866 cm^{-1}. The solvent was removed in vacuo and the resulting red solid was dissolved in a minimal amount of CH_2Cl_2. Hexanes were added to precipitate the residual magnesium salt and the red liquid was cannula filtered to another flask, where the solvent was removed in vacuo to yield a red solid. Column chromatography on silica with methylene chloride eluted a red band (24 mg, 60%). Complex **4** was dissolved in hexanes and placed in a freezer at −30 °C. Dark red crystals suitable for X-ray analysis formed after a few days. IR (hexanes): ν_{CO} = 1881, 1885 cm^{-1}. ^{1}H NMR (CD_2Cl_2, 298 K, δ, both diastereomers): 7.23–7.30 (m, 4H, *m*-C_6H_5), 7.13–7.15 (m, 2H, *o*-C_6H_5), 6.98–7.03 (m, 2H, *p*-C_6H_5), 6.75–6.77 (m, 2H, *o*-C_6H_5), 5.61, 5.55, 5.54, 5.52 (each a s, each 1H, acac C*H*), 3.85, 3.79 (each a s, each 3H, N−CH_3), 2.46, 2.43, 2.26, 2.17, 2.14, 2.10, 2.09, 2.06 (each a s, each 3H, acac CH_3), 2.45, 1.96 (each a s, each 3H, N=C−CH_3). ^{13}C{^{1}H} NMR (CD_2Cl_2, 298 K, δ, both diastereomers): 23.2, 24.6 (N=C−*C*H$_3$), 25.7, 26.0, 26.3, 26.8, 27.5, 27.6, 28.0, 28.1 (acac *C*H_3), 40.0, 40.7 (N−*C*H_3), 59.3, 60.6 (N−*C*), 99.4, 99.6, 101.1, 101.5 (acac *C*H), 126.2, 126.4 (*p*-C_6H_5), 126.3, 127.1, 127.2, 127.3 (*o*/*m*-C_6H_5), 149.7, 150.6 (*ipso*-C_6H_5), 185.2, 185.7, 185.7, 186.3, 186.4, 187.7, 193.9, 194.3 (acac *C*O), 234.6, 236.5 (*C*≡O). Anal. Calcd for $C_{20}H_{25}O_5NW$: C, 44.21; H, 4.65; N, 2.58. Found: C, 44.03 H, 4.49; N, 2.02.

W(CO)(acac)$_2$(η^2-EtN=CMe$_2$) (5). A 200-mL Schlenk flask was charged with **2c** (50 mg) and THF (25 mL). The resulting green solution was cooled to −78 °C. A solution of methylmagnesiumbromide (40 μL, 3 M in Et_2O) was added to the flask yielding a red-brown solution. Solvent was removed in vacuo after 1 h and the product was extracted with hexanes. Removal of solvent gave

a red-brown powder (30 mg, 69%). ^{1}H NMR (CD_2Cl_2, 298 K, δ): 5.58, 5.46 (each a s, each 1H, acac C*H*), 3.94 (m, 2H, N−CH_2−CH_3), 2.40, 2.15, 2.07, 1.99 (each a s, each 3H, acac CH_3), 2.20, 2.03 (each a s, each 3H, N−C(CH_3)−CH_3). ^{13}C{^{1}H} NMR (CD_2Cl_2, 298 K, δ): 16.4 (N−CH_2−*C*H_3), 26.1, 26.4, 27.3, 28.0 (acac *C*H_3), 30.0, 31.9 (N−C(*C*H_3)−*C*H_3), 49.6 (N−*C*H_2−CH_3), 59.8 (N−*C*), 99.5, 101.0 (acac *C*H), 185.6, 185.7, 186.2, 194.0 (acac *C*O), 233.6 (*C*≡O).

Acknowledgment. We thank the National Science Foundation (CHE-0717086) for financial support.

Supporting Information Available: Full details of the crystal structure analyses for **2a** and **4** in CIF format and NMR spectra of **2c**, **3b**, and **5**. This material is available free of charge via the Internet at http://pubs.acs.org.

OM7009039